Spitzer and HHT Observations of the Active Star-Forming Complex W51

Miju Kang[1], John H. Bieging[2], Craig A. Kulesa[2], Youngung Lee[1], Minho Choi[1], William L. Peters[2]
[1]International Center for Astrophysics, Korea Astronomy and Space Science Institute, South Korea
[2]Steward Observatory, University of Arizona, USA

CONTACT:

ABSTRACT: We present the results of an extensive observational study of the active star-forming complex W51. We observed this region in the *J=2-1* transition of the ^{12}CO and ^{13}CO molecules over a 1.25° x 1.00° region with the University of Arizona Heinrich Hertz Submillimeter Telescope. We use a statistical equilibrium code to estimate physical properties of the molecular gas. We compare the molecular cloud morphology with the distribution of infrared (IR) and radio continuum sources, and find associations between molecular clouds and young stellar objects (YSOs) listed in *Spitzer* IR catalogs. We estimate that about 1% of the cloud mass is currently in YSOs by comparing the total gas masses to total masses of YSOs in the active star-forming region of W51.

1. INTRODUCTION

Establishing the properties of molecular clouds is essential in understanding the formation and evolution of star-forming regions. Newly formed massive stars can affect the parental molecular clouds through ionization, heating, and expansion of the H II regions, stellar winds, and supernova-driven shocks. These mechanisms are either compressing or dispersing the surrounding clouds. For a better understanding of the feedback process in the interstellar medium (ISM), detailed observations of the molecular clouds and identification of embedded young stellar objects (YSOs) are required.

W51 is one of the most luminous star-forming regions in the first quadrant of the Galactic plane. The high luminosity comes from a large number of O-type stars that are within the molecular cloud.

2. OBSERVATIONS

2.1. ^{12}CO and ^{13}CO $J = 2 - 1$ and ^{13}CO $J = 1 - 0$

We present new observations of W51 in the $J = 2 - 1$ ^{12}CO and ^{13}CO lines with the 10 m Heinrich Hertz Telescope (HHT) on Mount Graham, Arizona. Our on-the-fly (OTF) maps are fully sampled in two lines simultaneously with an angular resolution of 32", and with an rms noise per velocity channel of ~0.1 K in antenna temperature.
We obtained ^{13}CO $J = 1 - 0$ data for the same region from the Galactic Ring Survey.

2.2. *Spitzer* Data

- GLIMPSE I (IRAC 3.6, 4.5, 5.8, and 8.0 μm)
- MIPSGAL (MIPS 24 μm)
- Kang et al. (2009b) identify and classify YSOs near the W51 H II region complex using spec

3. RESULTS

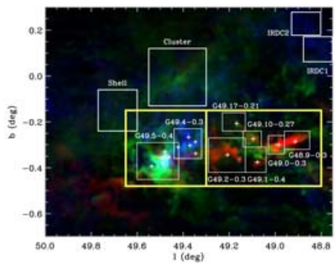

Figure 1

Color image of the W51 region composed of ^{12}CO $J = 2 - 1$ intensity integrated over the velocity range of 30-55 km s^{-1}, 56-65 km s^{-1}, and 66-85 km s^{-1}. Cross symbols represent the compact radio continuum sources listed by Koo (1997). White boxes are the area for estimating the physical parameters in Table 1.

Table 1
Physical Parameters[a]

Name[b]	Selected Area				Velocity Range[c]	Mass[d]	A_V[e]	$^{13}R_{2-1/1-0}$[f]	$^{13/12}R_{2-1}$[g]
	l_{min} (°)	l_{max} (°)	b_{min} (°)	b_{max} (°)	(km s^{-1})	(10^4 $M_\odot$)	(mag)		
G49.5-0.4	49.42	49.60	−0.45	−0.29	49-72	8.7	72	0.87	0.31
G49.4-0.3	49.32	49.44	−0.36	−0.23	47-55	3.7	26	1.01	0.26
G49.2-0.3	49.13	49.29	−0.42	−0.27	62-73	3.8	21	0.78	0.25
G49.1-0.4	49.04	49.13	−0.42	−0.31	56-76	1.6	20	0.98	0.23
G49.17-0.21	49.13	49.21	−0.24	−0.18	58-69	0.9	20	0.78	0.37
G49.10-0.27	49.06	49.14	−0.31	−0.24	58-70	1.3	22	0.83	0.25
G49.0-0.3	48.90	49.03	−0.34	−0.26	62-75	1.5	26	1.14	0.23
G48.9-0.3	48.85	48.96	−0.32	−0.24	63-74	1.9	26	1.16	0.20
Shell	49.60	49.77	−0.24	−0.06	55-68	2.9	15	0.43	0.12
Cluster	49.30	49.55	−0.13	0.12	59-69	6.0	15	0.41	0.13
IRDC1	48.75	48.88	0.06	0.17	47-56	1.7	14	0.54	0.17
IRDC2	48.80	48.93	0.18	0.28	42-49	1.1	9	0.52	0.17

Notes.
[a] We assumed a distance of 6 kpc from the Sun to derive the physical parameters.
[b] See Figure 1.
[c] Velocity range considered in the estimation of mass and line ratios.
[d] Mass derived using an LVG escape probability radiative transfer model.
[e] Peak A_V derived from the CO column density.
[f] Mean ^{13}CO $J = 2 - 1/J = 1 - 0$ intensity ratio.
[g] Mean ^{13}CO/^{12}CO $J = 2 - 1$ intensity ratio.

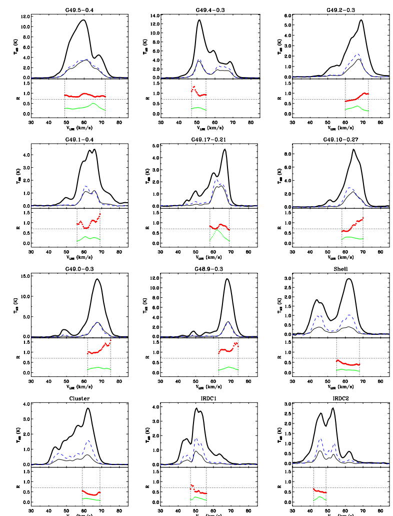

Figure 2

Average spectra of ^{12}CO $J = 2-1$ (thick line), ^{13}CO $J = 2-1$ (thin line), ^{13}CO $J = 1-0$ (dashed line) and $^{13}R_{2-1/1-0}$ (red crosses) and $^{13/12}R_{2-1}$ (green dots) for the boxed areas in Figure 1. Two vertical dotted lines show the velocity range for deriving mass and the average line ratio of clouds, as listed in Table 1. A typical uncertainty is smaller than the symbols.

Line Ratios

CO line ratios are useful indicators of trends in line opacity and gas column density or of molecular excitation.

The average $^{13}R_{2-1/1-0}$ ratios associated with all HII regions are greater than 0.7, which implies that these clouds are relatively warm and dense. In contrast, the ratios of $^{13}R_{2-1/1-0}$ for the molecular clouds outside the active star-forming region, where there are no known continuum sources, are smaller than 0.7.

Physical Parameters

We use a non-LTE statistical equilibrium treatment of the CO molecular excitation to study physical properties of the molecular cloud. We apply the escape probability radiative transfer and the photodissociation model to our ^{12}CO and ^{13}CO $J = 2-1$ data.

We adopt a distance of 6 kpc and use that value to calculate the gas masses of the selected regions shown in Figure 1. In Table 1, we list the size of the regions, velocity range, masses, extinctions, and the mean ratios of the lines.

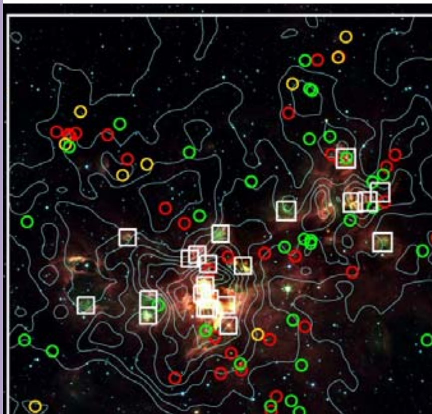

Figure 3 Color image of the **W51A** region composed of IRAC 5.8 μm (red), 4.5 μm (green), and 3.6 μm (blue). Contour map of ^{12}CO $J = 2-1$ intensity integrated from **45 to 65 km s^{-1}**. The contour levels are 40, 80, 120, 160, 200, 240, 280, 320, 360, and 400 K km s^{-1}. Squares are compact radio continuum sources listed by Mehringer (1994). YSO candidates (open circles) are marked in red for Stage 0/I, yellow for Stage II, and green for ambiguous sources.

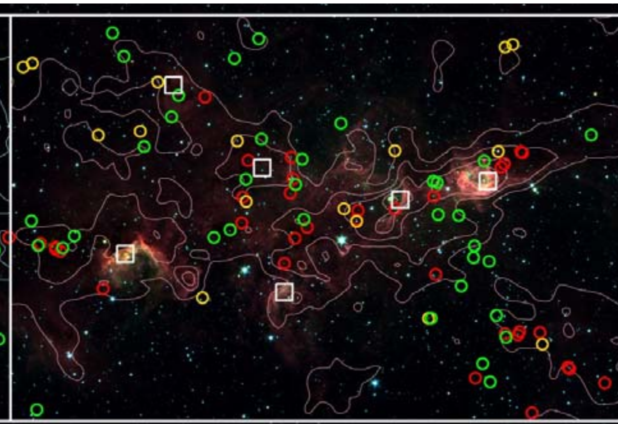

Figure 4 Color image of the **W51B** region composed of IRAC 5.8 μm (red), 4.5 μm (green), and 3.6 μm (blue). Contour map of ^{12}CO $J = 2-1$ intensity integrated from **55 to 75 km s^{-1}**. The contour levels are 30, 90, 150, 210, and 270 K km s^{-1}. Squares are compact radio continuum sources listed by Koo (1997). YSO candidates (open circles) are marked in red for Stage 0/I, yellow for Stage II, and green for ambiguous sources.

4. SUMMARY

1. CO emission in the 1.25° × 1.00° area divides into three velocity components, 30-55, 56-65, and 66-85 km s^{-1}. G49.4-0.3 and some clouds in the northwestern part of the map are associated with the lower velocity (30-55 km s^{-1}) component. The main molecular clouds in the velocity range of 56-65 km s^{-1} are distributed widely throughout the whole region. The higher velocity component (>66 km s^{-1}) shows an elongated filamentary structure from southeast to northwest.

2. The average ratios of $^{13}R_{2-1/1-0}$ and $^{13/12}R_{2-1}$ of all H II regions are greater than the values outside the active star-forming regions, which implies that the molecular gas directly associated with the H II regions is dense and highly excited.

3. We compare our CO maps with *Spitzer* data. Strong PAH emission near H II regions seen in IRAC bands coincides with bright CO emission, suggesting that those molecular clouds are associated with the H II regions. Many YSOs are detected in the dark parts near the H II regions on IRAC images.

4. We estimate the total gas masses of the various interesting regions using an LVG analysis of ^{12}CO and ^{13}CO $J = 2 - 1$ data. By comparing the total gas mass to total mass of YSOs in W51A and W51B, we find current YSO formation efficiencies of 0.7% and 1.1%, respectively, within a timescale of 3 × 10^4 yr during which massive stars (>5 $M_\odot$) would be detected as YSOs. The *current* rate of star formation in the W51 GMC should then be an order of magnitude higher than the rate averaged over an assumed cloud lifetime of 3 × 10^6 yr, in order to convert 10% of the cloud mass to stars.

Triggered Star Formation

We argue that triggered star formation resulted from H II region expansion into clouds in the shell structure near W51A (Kang et al. 2009a) and in the region around G49.0-0.3 and G48.9-0.3. We also present evidence of star formation triggered by cloud-cloud collisions in G49.5-0.4 and G49.17-0.21.

References

Merhringer, D. M. 1994, ApJS, 91, 713
Kang, M., Bieging, J. H., Kulesa, C. A., & Lee, Y. 2009a, ApJ, 701, 454
Kang, M., Bieging, J. H., Povich, M. S., & Lee, Y. 2009b, ApJ, 706, 83
Koo, B.-C., & Moon, D.-S. 1997, 475, 194

MORE INFO

Kang et al. (2010) ApJS, 190, 58